Unequal intralayer coupling in a bilayer driven lattice gas

Choon-Peng Chng and Jian-Sheng Wang
Department of Computational Science, National University of Singapore, Singapore 119260, Republic of Singapore
(Received 2 November 1999; revised manuscript received 7 February 2000)

The system under study is a twin-layered lattice gas at half filling, being driven to nonequilibrium steady states by a large, finite ''electric'' field. By making intralayer couplings unequal, we were able to extend the phase diagram obtained by Hill, Zia, and Schmittmann and found some interesting effects. Many transient phases to the strip phase were found to be long lived. We also attempted to test whether the driven lattice gas with negative interlayer coupling is still in the Ising universality class. Simulation results suggest a value of 1.75 for the exponent γ but a value closer to 2.0 for the ratio γ/ν. We suspect a different susceptibility has to be used due to the presence of two phases near criticality.

PACS number(s): 05.50.+q, 64.60.Cn, 05.70.Jk

I. INTRODUCTION

Equilibrium statistical mechanics has served us well in the understanding of collective behavior in many-body systems in, or near, thermal equilibrium. However, nature abounds with examples of systems that are far from equilibrium and their behavior cannot be predicted by theory. Linear response theory, a form of perturbation theory, works well only for systems slightly off equilibrium but not for those far from equilibrium. The way to tackle such new systems is to study simple models that have well-understood equilibrium properties.

Much work has followed from the early attempt by Katz, Lebowitz, and Spohn (KLS) [1] to drive the Ising lattice gas into nonequilibrium steady states via the introduction of an external electric field. This driven lattice gas (DLG) model became the prototype for studying driven diffusive systems (DDSs).

The KLS or standard model for a DDS is composed of an ordinary lattice gas in contact with a thermal bath, involving particles hopping to their nearest unoccupied sites. This is controlled by a rate specified by both the energetics of interparticle interactions and an external, uniform driving field [2].

Achahbar and Marro [3] studied a variant of the standard model: stacking two fully periodic standard models on top of one another, without interactions across the layers. This system is coupled to a heat bath at temperature T using spin-exchange (Kawasaki) dynamics with the usual Metropolis rate. In Kawasaki dynamics, pairs of sites (both intra- and interlayer) are considered for exchange in order to have global conservation of particles. Thus we have a diffusive system without sources or sinks. Half-filled systems are studied. The two decoupled Ising systems undergo two phase transitions as the temperature is decreased from a large value. First, the disordered (D) phase at high T transforms into a state with strips in both layers (S phase). This is much like two aligned, single-layer driven systems. Upon further lowering of T, another transition occurs that results in an ordered state, resembling the equilibrium Ising system. It consists of a homogeneously filled layer and an empty layer [filled-empty (FE) phase].

Hill, Zia, and Schmittmann [4] unveiled the mystery of the presence of two phase transitions. They did a natural extension to Achahbar and Marro's model: addition of a coupling across the layers. This coupling, J_z (J in their notation), can be both attractive and repulsive. This led to novel discoveries. From the new phase diagram in T-J_z space at fixed E, they observed the intrusion of the region of the S phase into that of the FE phase. The reader is referred to their paper for the phase diagram. The ''usual'' FE to D transition is interrupted by the presence of the S phase for very small and negative J_z as well as at $J_z=0$. Note that a large but finite electric field E is used to drive the system far out of equilibrium.

In our paper, we investigate such systems further with yet another trivial modification. We attempt to observe the effects of having an unequal coupling in the x and y directions within each top and bottom layer. In particular, we wish to map out the phase diagram in the T-J_z-J_y plane. Taking **E** to be in the x direction, we have particle-particle interactions in the transverse direction, J_y, that are larger than or equal to those along the field, J_x. The case of equal interactions should recover the results in [4].

In addition to extending the phase diagram into another dimension, we also attempt to determine the universality class of the system for $J_z<0$, i.e., for FE to D second-order transitions. It was stated in [4] that preliminary results seem to suggest that the D-S transition belongs to the class of *single-layer driven lattice gases*. It is our objective here to test the hypothesis that the D-FE transition belongs to the *Ising* universality class, to which many systems belong.

II. DEFINITION OF THE MODEL AND TOOLS EMPLOYED

Following Hill *et al.*, our system consists of two fully periodic $L\times L$ square lattices, arranged in a bilayer structure. We label the sites by (j_1,j_2,j_3) with $j_1,j_2=0,\ldots,L-1$ and $j_3=0,1$. Each site may be either occupied or empty, such that we can specify a configuration of the system by a set of occupation numbers $\{n(j_1,j_2,j_3)\}$, where n is 0 or 1. In spin language, we have spin $s=2n-1=\pm 1$. For half-filled systems, $\Sigma n=L^2$ or $\Sigma s=0$, i.e., zero net magnetization. The Hamiltonian is given by

$$H=-J_1\sum_{x\ dir} nn'-J_2\sum_{y\ dir} nn'-J_3\sum nn'', \qquad (1)$$

where n and n' are the occupancies for nearest neighbors within a given layer while n,n'' are for those across layers. Summations in the x and y directions include both top and bottom layers. From now on, $J_{1,2,3}$ will be used in place of $J_{x,y,z}$.

Note that with $J_3=0$, we have two decoupled Ising systems. This has been confirmed by computing the equivalent Ising model heat capacity from the system and comparing with exact results, where good agreement is observed. We restrict J_1 and J_2 to positive values and shall define the dimensionless couplings $\alpha=J_2/J_1$ and $\beta=J_3/J_1$ for numerical convenience. We took β in the range $[-10,10]$ while α took on values 1, 2, 5, and 10. With $\alpha=1$, we hope to reproduce the results obtained by Hill *et al.*

The temperature T is given in units of the single-layer Onsager temperature, $0.5673J_1/k_B$ in particle language. Finally, the external driving field E is given in units of J_1 as well, which affects the Metropolis rate via a subtraction of E from $\triangle H$ for hops along the field, and vice versa. A value of 25 is used throughout the study.

Lattices investigated are of dimensions $L=32$, 64, and 128. Typical Monte Carlo steps (MCS) per site taken are 500 000 for the phase diagram determination and 10^6 for the universality class investigation. Runs are performed at fixed α, β, E, and T (all dimensionless), starting from a random initial configuration generated by a 64-bit linear congruential random number generator. Discarding the first 5×10^4 MCS (for transients), measurements are taken every 200 MCS. However, if a significant change in character is seen in the configuration, as in any approach to the true steady state from any local minimum (in energy), the time average is taken only after the changeover point.

To determine the critical temperatures, many systems are started from identical initial states but with different T's. A susceptibility plot is then constructed from which the T value giving the maximum susceptibility (T_{peak}) is obtained via a quadratic least-squares fit. This is to be repeated for each L and the estimate for T_c obtained via the usual finite-size scaling hypothesis,

$$T_{peak}(L)-T_c\propto L^{-1/\nu}. \tag{2}$$

The critical exponent ν is chosen to be 1.0 (tentatively), as for the Ising model. In fact, for an undriven system with $\alpha=1$ and $\beta=0$, the T_c obtained via this method is 0.9886, using $L=4$, 8, 16, and 32. This is in good agreement with the expected value of 1.0. However, for a driven system, it has yet to be shown explicitly that ν is still 1.0, which is the other objective of this paper.

For the D-S transitions, it was suggested in [5] that the critical exponent ν is 0.7. Nonetheless, due to the enormous demand on computer time, T_{peak} is taken as a rough estimate for T_c in the determination of the phase diagrams. Thus for D-FE transition the T_{peak} values serve as upper bounds on the true critical temperatures. Hence the exact value of ν should not affect the phase diagrams significantly.

The susceptibility is defined as

$$\chi(l_1,l_2,l_3)=\frac{L^d}{k_BT}[\langle|\tilde{n}(l_1,l_2,l_3)|^2\rangle-\langle|\tilde{n}(l_1,l_2,l_3)|\rangle^2], \tag{3}$$

where $k_B=1$ and $d=2$ for our two-dimensional (2D) system and $\langle|\tilde{n}|\rangle$ is taken to be the relevant order parameter. We define $\{l_1,l_2,l_3\}$ as taking the same range as $\{j_1,j_2,j_3\}$ introduced earlier. The Fourier transform of the occupancy $n(j_1,j_2,j_3)$ is given by

$$\tilde{n}(l_1,l_2,l_3)=\frac{1}{2L^2}\sum_{j_1,j_2,j_3} n(j_1,j_2,j_3)e^{2\pi i[(j_1l_1+j_2l_2)/L+j_3l_3/2]}. \tag{4}$$

Thus, in order for the fast Fourier transform to be applicable, only the system sizes $L=2^p$ are used, with p being any positive integer.

The quantity $S(l_1,l_2,l_3)=\langle|\tilde{n}(l_1,l_2,l_3)|^2\rangle$ is called the *structure factor*. Different pure phases are represented by different structure factors and the deviation of each from the maximum value measures the presence of each of these phases in a given configuration. A change across the lattices is reflected in the third index l_3 in $\tilde{n}(0,0,1)$. For a pure FE phase, $|\tilde{n}(0,0,1)|^2=0.5^2=0.25$ is the only nontrivial positive entry in the power spectrum [besides the trivial $|\tilde{n}(0,0,0)|^2=0.25$ due to the half-filled nature of the lattice]. For a phase that is 90% FE-like, the value will be slightly less than 0.25. Thus the quantity $S(0,0,1)$ computed is the structure factor for the pure FE phase, where the time average operations are redundant for the pure phases. Other entries in the power spectrum such as $|\tilde{n}(0,1,0)|^2$ can be used to characterize other phases. In fact, Hill *et al.* used this entry's time average $S(0,1,0)$ to represent the S phase, but we found that any odd l_2 index suffices.

We thus speculate that any given configuration of the bilayer DLG can be viewed as consisting of a superposition of many ''pure tones,'' such as the FE configuration. Thus, through a Fourier transform, we can pick out the ''frequencies'' present by monitoring a few entries in the power spectrum that represent various possible steady states from energy arguments. Upon taking time averages, the corresponding structure factors can be computed. For D-FE transitions, $S(0,0,1)$ is monitored together with $S(0,1,1)$, which represents the ''local minimum'' solution. This is a staggered form of the FE phase, with an occupied band on

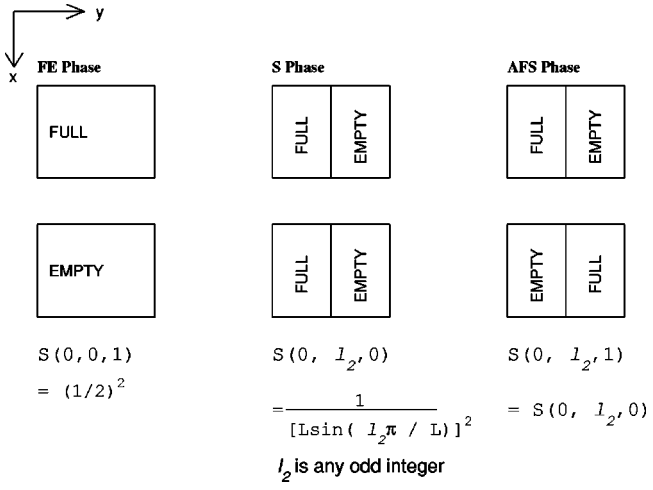

FIG. 1. The pure configurations: FE, S, and AFS phases.

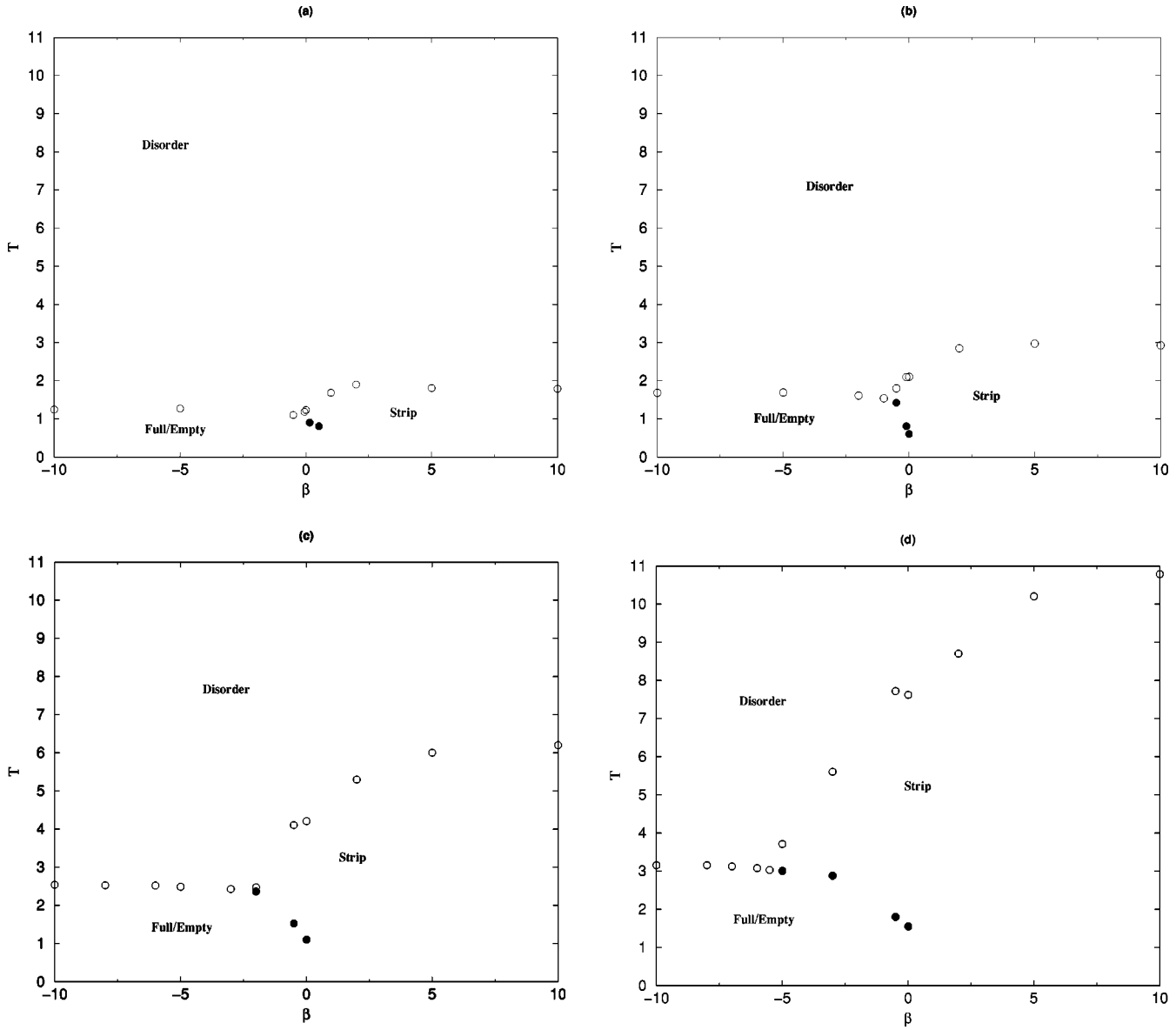

FIG. 2. Phase diagrams for the bilayer lattice gas: (a) $\alpha=1$, (b) $\alpha=2$, (c) $\alpha=5$, and (d) $\alpha=10$.

one layer matched by an empty one on the other. We termed this the AFS (antiferromagnetic strip) phase. It is like a hybrid between FE and S phases and occurs at low temperatures for systems with repulsive interlayer coupling (see Fig. 1 for a pictorial view). The transition from a pure FE phase (dominant at moderate temperatures) to disorder is marked by a drop of $S(0,0,1)$ from its maximum of 0.25 to near zero. The location of T_c is where the slope of the drop is the largest or where $\chi(0,0,1)$ peaks.

Due to finite-size effects, the peaks of the susceptibility function do not diverge to infinity but the distribution is ''rounded'' and the peak location shifted in temperature. These two features are observed in our simulation data.

III. PHASE DIAGRAMS

The phase diagram for a driven system with the same parameters as used by Hill *et al.* can be reproduced to an acceptable degree by our implementation. We shall present our phase diagrams (Fig. 2) as slices off the full 3D phase diagram in the T-β-α space.

A few qualitative features can be discerned from the phase diagrams. The first of these is the growth of the ''triangular'' region, a term coined in Hill's paper for the intrusion region of the S phase into that for the FE phase, as α is increased. This observation provides an independent confirmation of the existence of this phenomenon. Without an external drive, no bias exists between the FE and the S phases. However, application of a drive in the x direction (vertical) seems to favor the S phase, with its linear interface aligned with the drive, as compared to the isotropic FE phase. This is speculated to be analogous to magnetic domain growth in a ferromagnetic material under the action of an external magnetic field. The S phase, which is not expected to be stable when repulsive interactions exist between the layers, could become stable due to the drive. The driving field could somehow compensate for the gain in configuration energy as a result of particle stacking under repulsive interactions. The survival of the S phase in the negative β region is increased as α increases.

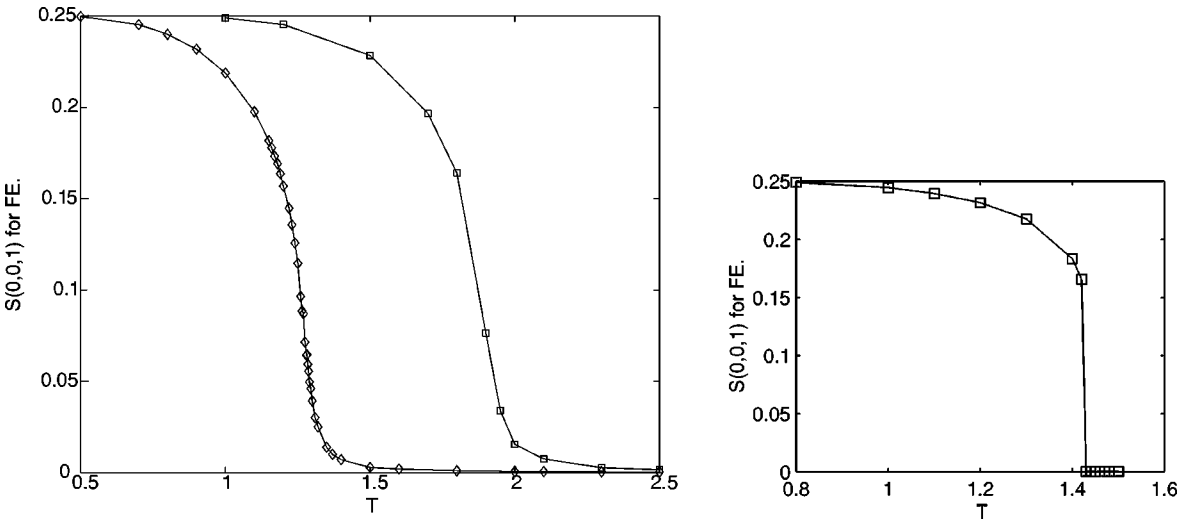

FIG. 3. Plots of structure factor $S(0,0,1)$ (for FE) against T. The left figure is for $\alpha=1$, $\beta=-5$, $L=32$, and $E=0$ ($\square$) which is an example of a second-order transition. Also shown on the same plot is the driven case, $E_x=25$ ($\diamondsuit$). On the other hand, the right figure serves as an illustration of the structure factor discontinuity at a first order transition and is obtained at $\alpha=2$, $\beta=-0.5$ and same L, E_x values.

Another feature worth noting is the shifting of the bicritical point toward more negative β values as well as toward higher temperatures. Thus the S phase becomes more stable at moderate β values as α is increased, despite its instability from energy arguments.

We judge whether the transition is second or first order by looking at the plots of structure factors against temperature T. A second-order transition has continuous derivatives at every point, an example of which is shown in Fig. 3 for the D-FE transition. A first-order transition, like FE-S in the second figure, will show a discontinuity.

Table I presents some representative T_c values from the phase diagrams. One can plot the difference between the T_c values for the second- (D-S) [column 4 of the table: 0.0(2)] and first- (S-FE) [column 3 of the table] order transitions along the $\beta = 0$ line against α and observe that a least-squares straight line can be fitted through them. However, due to a lack of finite-size scaling knowledge for the D-S transition, we could not get a better estimate for T_c at the second-order transition point and thus could not conclude if the error bars could tolerate a linear fit. Nonetheless, a linear fit might be possible, though no theory has yet been developed to investigate this.

We also plotted T_c at $\beta=-10$, 0, and 10 against the α values. The plot for $\beta=-10$ (D-FE) seems to exhibit a logarithmic relationship. As for the non-negative β values, which are for D-S transitions, the relationship seems linear except at large α for $\beta=10$ and small α for $\beta=0$.

TABLE I. Critical temperatures at three selected β values.

α	β			
	-10.0	0.0 (1)	0.0 (2)	10.0
1.0	1.242	$\sim$0.950	1.228	1.781
2.0	1.692	0.600	2.100	2.923
5.0	2.535	1.100	4.205	6.200
10.0	3.152	1.550	7.619	10.779

IV. INTERPRETATION AND DISCUSSION OF PHASE DIAGRAMS

The survival of the FE phase under a driving field should not be taken as to be expected. For large α, we would expect staggered and horizontal antiferromagnetic bands to form in the undriven bilayer LG from energy arguments. The form looks like the AFS configuration but rotated 90°. Under a driving field directed perpendicular to these bands, it appears that even a large coupling of 10 could not stand up to the effect of an even larger driving field (strength 25). It has yet to be seen if the reverse situation can favor the rotated AFS phase.

We can try to interpret the phase diagrams as follows. First, the increased intrusion of the S phase as α increases can be understood through a thought experiment. The S phase can be thought of as consisting of strings of particles, of one particle width, aligned with the driving field. These are bounded together through the coupling α, in the transverse direction to the field $E\hat{x}$. As T increases, the arrangement will be disturbed until, at a sufficiently large T, disorder reigns. However, if we increase α, the increased binding could compensate for the disorienting effect of large T. This effectively makes the critical temperature for the S-D transition higher.

However, this is not to say that the increased α does not help to increase T_c for the D-FE transitions as well. It is only that the increase is much smaller in the FE case.

The effect of α is to help neighboring particles to bind together in the y direction. This helps the configuration to hold together despite the larger temperatures applied and is true for both S and FE phases. One possible reason for the much lower thermal tolerance for the FE case might be that each of the L^2 particles in one layer has equal probability to leave the pure FE phase. On the other hand, for the S phase, only particles at the edges (for top and bottom layers)

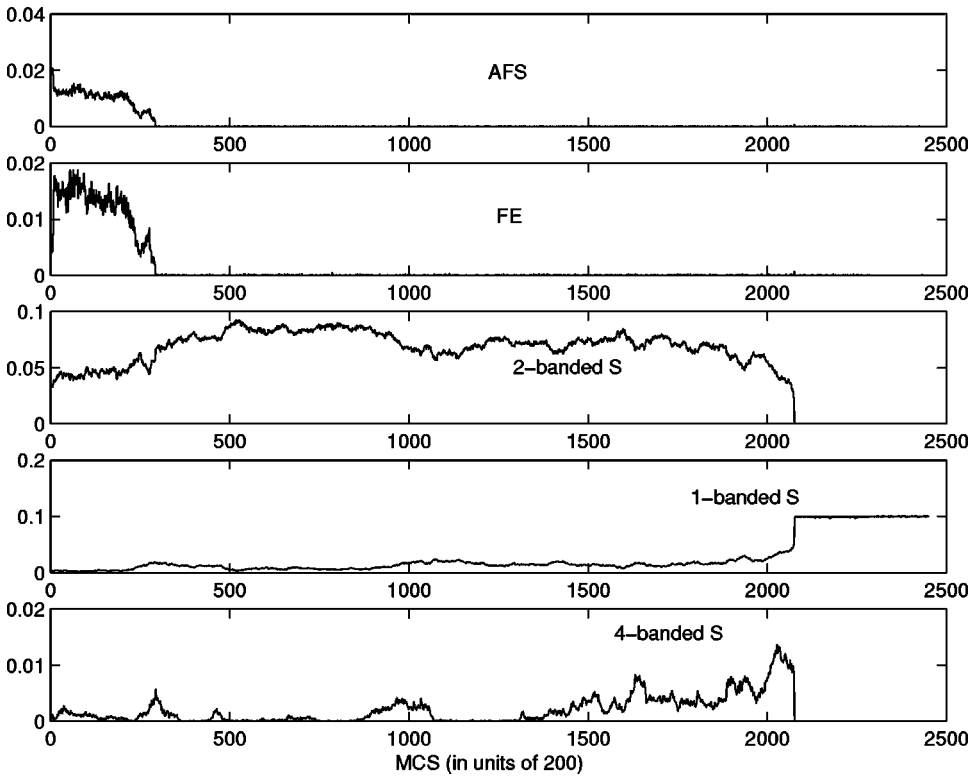

FIG. 4. Example illustrating the two-banded S as a transient to the final one-banded S phase. This is typical of systems with large α and well inside the intrusion region at negative β, with temperatures well above the S-FE transition line but less than those values that give very fast convergence to the single-banded S phase. The entries in the power spectrum monitored are (0,1,1) for AFS, (0,0,1) for FE, (0,2,0) for two-banded S, (0,1,0) for one-banded S, and (0,4,0) for four-banded S phase. The run-time averages taken produce the structure factors for each case. Note that the maximum values for $|\tilde{n}(0,2,0)|^2$ and $|\tilde{n}(0,1,0)|^2$ are both 0.1016 for the case of $L=32$.

aligned with the field can migrate transverse to the field and leave the pure S phase. This implies that only $O(L)$ particles have a chance of migration. Thus it is easier to destroy a FE phase than an S phase once they are formed. In actual simulations starting from random configurations, this implies that it is easier to form the S phase. This might provide the key to the stark difference in the amount of benefit acquired from an increased α for the two pure phases. The argument also holds for configurations of a ''near FE'' or ''near S'' nature, before the critical temperature.

Further, each movement of a particle out of the filled band for an S phase violates the occupied-occupied single-site configuration across the layers, which is typical of the S phase. However, the exchange of a particle with a hole on the opposite layer in a FE phase does not violate the empty-occupied configuration typical of an FE phase. Note that this argument is only for a single site. Hence in a way it is easier to destroy an FE phase.

Conversely, starting from an initial random configuration, it is harder to form the FE phase as particles must not just couple together, they must all reside on one of the layers. This can only happen at low enough T. Thus we may argue that the FE phase is the dominant phase only at large enough repulsive interlayer couplings under the drive.

V. LONG-LIVED TRANSIENTS

When investigating the transition of the FE to S phase (first order due to a discontinuity in the structure factor versus T plot), several *transient* phases are observed. They appear to be the ''local minimum'' solutions of an optimization problem in which the S phase is the best solution, i.e., the configuration of lowest free energy satisfying the parameters of the system.

The transient phases observed are composed of from two up to four or five vertical bands, compared to the S phase which has only one band. These are dominant at the comparatively low T for the FE-S transition, whereas we can find the S phase again at moderate T. In fact, these multibanded structures has also been reported recently by Zia *et al.* [6] based on an anisotropic DLG model investigated in [7]. The structures were also seen in an anisotropic lattice gas automata model proposed by Marro *et al.* in [8]. In the latter case, they have a single lattice gas system evolving under not the Metropolis rate but automata rules.

The n-banded S phases are seen to give way to the two-banded phase as T increases. For certain runs at moderate T, the latter is even seen to ''evolve'' into the single-banded phase during a long enough simulation run (more than 3×10^5 MCS for $L=32$), as in Fig. 4. This observation lends further evidence that the n-banded phases are the local minima, from which we could reach the global minimum with an increase in T or a longer run.

Here, we can also speculate that the cause of the emergence of n-banded S phases is the larger coupling α. In [8], the n-banded S phases were obtained with a setting of 0.9 for a parameter b in their model, with $b\in[0,1]$. If $b>1/2$, this implies that there exists a tendency for particles to approach each other in the direction transverse to the driving field. For $b<1/2$, it represents a tendency for particles to separate from each other. Thus we can see that $b=0.9$ has a similar effect to a large α in our case. This realization implies that the n- to single-banded S phase transition is a real phenomenon in DDSs as it can be produced by different models.

The transients were not reported in Hill's work, probably because the ratio α is 1. Only when the coupling in the transverse direction to the drive increases far beyond 1 can these transients be observed. The increase of α has the effect of ''stretching out'' the system dynamics, making otherwise

short or nonexistent transient phenomena emerge. In fact, we observed that structure factor plots for the same parameter settings are similar in form for $\alpha=1$ and $\alpha=10$ except that the temperature range is 10 times larger for the latter α value.

Finally, some words about obtaining the FE-S first-order transition line. For $\alpha>1$, the FE phase is seldom observed inside the ''triangular'' region. Instead, either the AFS phase or a *mixed phase* having both AFS and *n*-banded S characteristics is observed. This then leads to the *n*-banded S phase at higher *T*. Thus we are seeing another transient configuration. Their appearance effectively hid the first-order transition line and so a heuristic approach has to be taken. We simply take the smallest *T* that gives an *n*-banded S phase as an estimate of T_c(FE-S).

VI. CRITICAL EXPONENT DETERMINATION

In the literature, there is some work on the universality class of bilayered systems by Marro *et al.* [5]. In their paper, they looked at systems with no interlayer coupling and found that the S-FE transition belongs to the Ising universality class for $E<E_c\approx 2$, due to the presence of a tricritical point. As we used a value of E much larger than E_c, we observed a first-order transition instead. The D-FE transition is not observable in the absence of interlayer coupling under a drive.

To the authors' knowledge, no work that reports on the universality class of the D-FE transition for an energetically coupled bilayer DLG exists in the literature. Here we tried to determine for a system under a finite but large drive. Working under the hypothesis that the system is Ising, we computed the quantity γ/ν to see if the Ising value of 7/4 could be obtained. This is done by assuming the finite-size scaling relation $\chi_{max}(L)\propto L^{\gamma/\nu}$.

Hence, by getting good estimates of the susceptibility peak values for various system sizes, we can obtain an estimate for the ratio γ/ν. The value of the exponent γ for the 2D Ising model is 7/4. As for ν, it is the correlation length exponent and takes on the value 1 for the Ising model.

Let us outline the tactic we used. For a given α setting, we attempt to obtain estimates of γ/ν as well as the individual exponents γ and ν for representative β values, namely, -1, -5, and -10. To do this, we require more detailed susceptibility plots especially for the region near the peak, where systems with *T* values differing only in the third decimal place are investigated. Data points close to the peak are fitted with a least-squares degree 2 polynomial and the maximum value as well as its location determined. These are the $\chi_{max}(L)$ and $T_{peak}(L)$ we desire. By repeating the procedure for system sizes $L=32$, 64, and 128, we could plot T_{peak} vs L with a guess for ν to obtain T_c.

By plotting $\ln\chi_{max}$ vs $\ln L$, the gradient of the least-squares fit straight line gives the ratio γ/ν. Now, the exponent ν becomes a free variable. For consistency in the plot of $\ln(\chi L^{-\gamma/\nu})$ versus $\ln(|T-T_c|L^{-1/\nu})$, we could either use $\nu=1$ or, assuming γ to be 1.75, obtain an ''experimental'' value for ν to be used for the determination of T_c. Thus we can have two sets of ''scaling'' plots. With these we can check to see if the derived quantities give good ''data collapse,'' which is expected if the scaling relations are satisfied. From the plot, the slopes of the two best-fit straight lines is expected to give us the exponent γ.

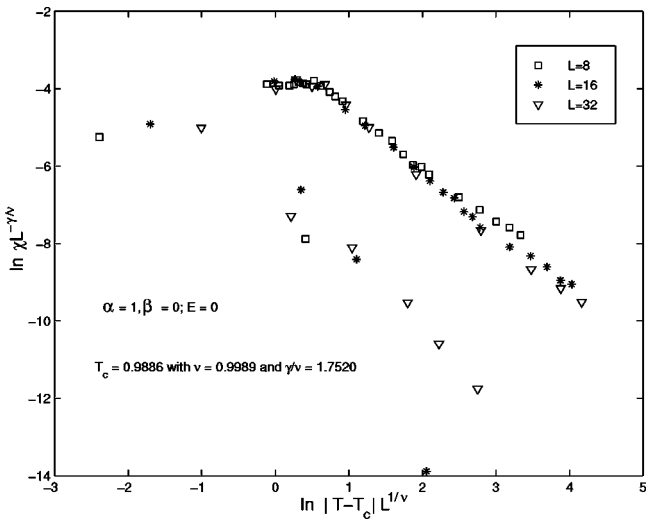

FIG. 5. Data collapse plot for the case of $\alpha=1$, $\beta=0$, and $E=0$ using all experimental values.

For a test of the method, we looked at the decoupled, undriven, and isotropic case, essentially expecting to see Ising behavior. With simulation runs of 5×10^5 MCS, the $T_{peak}(L)$'s for $L=8$, 16, and 32 are plotted against $L^{1/\nu}$, yielding a T_c of 0.9729 for $\nu=1$.

From the gradient of the $\ln\chi_{max}$ vs $\ln L$ plot, an estimate of 1.7520 is obtained for γ/ν. Assuming the exponent γ to be 1.75, we obtained the experimentally obtained ν value of 0.9989. We could also use this value of ν to return us a T_c of 0.9886. Hence, both cases give T_c very close to the expected value of 1.0 and we have self-consistency.

Looking at the scaling plot, Fig. 5, the value of γ is estimated from the slope of the least-squares fit line through the upper data points. This turns out to be 1.7273 for the cases of $[\nu=1.0, T_c=0.9885]$ and $[0.9989, 0.9886]$, using the same γ/ν of 1.7520 and assuming $\gamma=1.75$. Hence the method proposed is workable though slightly limited in accuracy.

With this much groundwork done, we can proceed to our findings. Due to time and resource constraints, only $\alpha=1$ and a portion of the $\alpha=2$ D-FE phase space is explored to determine the universality class. As a rough guide, the CPU time spent on this portion of the paper was about 1800 h (an underestimate) for a Digital Alpha processor running at 600 MHz. Typical running times are 1 h for $L=32$, 5 h for $L=64$, and 24 h for $L=128$, all with a run length of 1×10^6 MCS. All runs were started from the same initial (randomly) half-filled configuration but at different temperatures. Due to this, the maximum system size investigated is limited to $2\times128\times128$.

Figure 6 depicts the problems we faced in the determination of the peaks for the susceptibility plots. Data points are scattered about some fitting quadratic polynomial near the peak (''rounded''). An estimate of how well the polynomial fits the data values is needed to give a feeling of the error associated with the maximum χ value obtained via the fit.

We associate an error with the estimate of χ_{max} through the following heuristic approach. From the set of data points about the observed peak of the function, a linear interpolation is made to obtain more points. The difference between

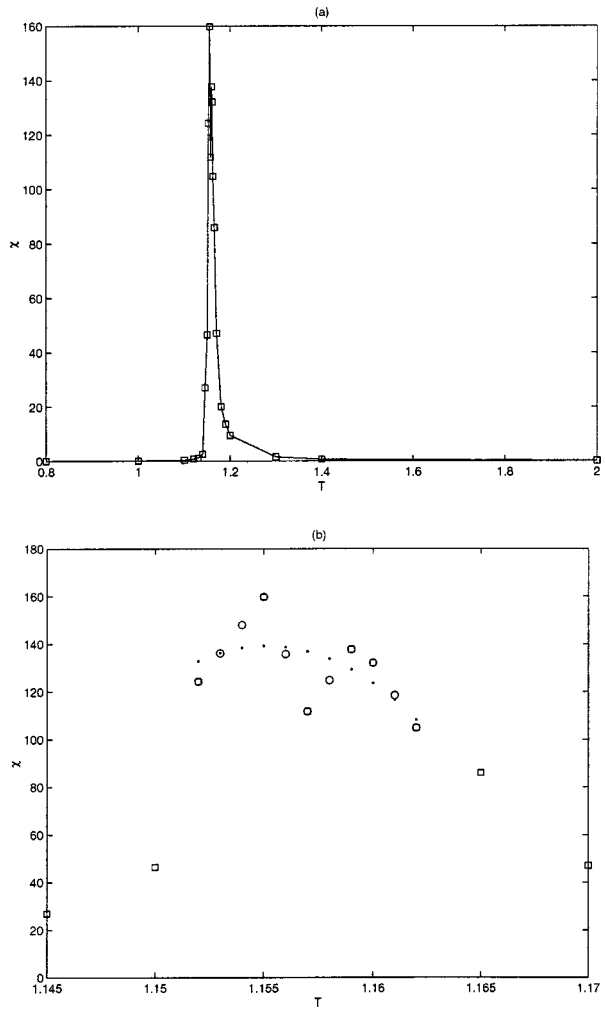

FIG. 6. Plots of χ against T for $\alpha=1$ and $\beta=-1$, with (a) being the full plot and (b) giving a zoomed-in picture. The simulation data are shown as squares while the dots in the second figure represent the attempt to fit a quadratic curve through the interpolated values. The circles are artificial data points generated by linear interpolation between the experimental data points in order to improve the eventual quadratic fit.

these pseudo data points and those from the parabolic fit to the chosen interval is denoted by ϵ $(=y_{data}-y_{fit})$. We next compute the variance of the set of ϵ values as $\mathrm{var}(\epsilon)=\langle\epsilon^2\rangle$ and take the standard deviation, $\sigma(\epsilon)=\sqrt{\mathrm{var}(\epsilon)/(n-1)}$ as an estimate of the error in χ_{max}. This gives us a gauge as to the spread of the ''errors'' when the data points are fitted by a least-squares degree 2 polynomial. However, this estimate does not tell us how far our estimate is from the true χ_{max} for the set of parameters, as effects like critical slowing down may be present to alter the observed peak height.

Making $\ln\chi_{max}$ versus L plots with error bars, we found that although the errors for $L=128$ are largest, they provide only little variation for the slopes of the best-fit straight lines.

Table II lists the estimates for the ratio γ/ν based on taking the ratio of $\ln(\chi_2/\chi_1)$ over $\ln(L_2/L_1)$, where the third entries for each β are the same as those obtained via least-squares fit gradients to $\ln\chi_{max}$ vs $\ln L$ plots. Here χ_1 is the short form of χ_{max1} for system size L_1. Listed are the values for different ratios L_2/L_1 as well as the propagated error in γ/ν, which is $\delta(\gamma/\nu)=[1/\ln(L_2/L_1)][\sigma(\epsilon)_2/\chi_2+\sigma(\epsilon)_1/\chi_1]$.

TABLE II. Values of γ/ν computed from various scenarios, with the associated errors. Also included are the intervals for various estimates of the ratios.

β	L_2/L_1	γ/ν	$\delta(\gamma/\nu)$	$\frac{\gamma}{\nu}-\delta\left(\frac{\gamma}{\nu}\right)$	$\frac{\gamma}{\nu}+\delta\left(\frac{\gamma}{\nu}\right)$
-1	64/32	1.846	0.026	1.819	1.872
	128/64	2.009	0.062	1.946	2.071
	128/32	1.927	0.020	1.907	1.947
-2	64/32	1.898	0.011	1.887	1.909
	128/64	2.084	0.056	2.029	2.140
	128/32	1.991	0.004	1.987	1.995
-5	64/32	1.774	0.015	1.759	1.789
	128/64	2.363	0.053	2.309	2.416
	128/32	2.068	0.027	2.042	2.095
-10	64/32	1.848	0.016	1.832	1.863
	128/64	2.191	0.030	2.161	2.221
	128/32	2.019	0.013	2.007	2.032

From Table II, it is clear that all intervals for γ/ν computed do not include the value 1.75. An important observation is that for ratios computed using the $L=128$ data, a value greater than 2.0 can be obtained. These data do not fit into our scheme of things so far, which places a limit that γ/ν is less than 2.

If we take the upper bound of the ratio γ/ν to be 2.0, the data points for $L=128$ may be inaccurate. As the errors computed could not explain the discrepancy, it was suspected that critical slowing down is quite severe in such a large system size and that the 1 million MCS taken was not sufficient for the system to reach the true steady state. If this is indeed the case, then the data for $L=32$ and 64 should be more trustworthy. But their intervals also do not include 1.75. Thus it is concluded that we observe here a significant deviation from the Ising value.

With the experimental ratios of γ/ν, we assumed γ to remain at the Ising 1.75 value and plotted T_{peak} against $L^{-1/\nu}$ for each setting of coupling strengths investigated. With ν less than or equal to 1.0, the plots obtained could not be well fitted with least-squares straight lines. In fact, all plots seem more logarithmiclike (i.e., concave functions). Is this another signature of a non-Ising system or the existence of two correlation lengths? We could not provide an answer at this current stage of research.

We made ''scaling plots'' for the different system sizes for each value of the parameter β investigated. With γ assumed to be 1.75 and $\gamma/\nu>1.75$ from simulation data, the ν computed will be less than 1.0. Scaling plots are made with ν set to 1.0 as well as the computed value and compared for the degree of data collapse, as well as observing whether the slopes of the upper and lower best-fit straight lines give the γ value assumed. It was found that the ''Ising'' plots were not consistent in that we do not recover the assumed γ value of 1.75 from the slopes. There are altogether eight plots for the four β settings we looked at (with $\alpha=1$).

From the scaling plots with the experimental values, we

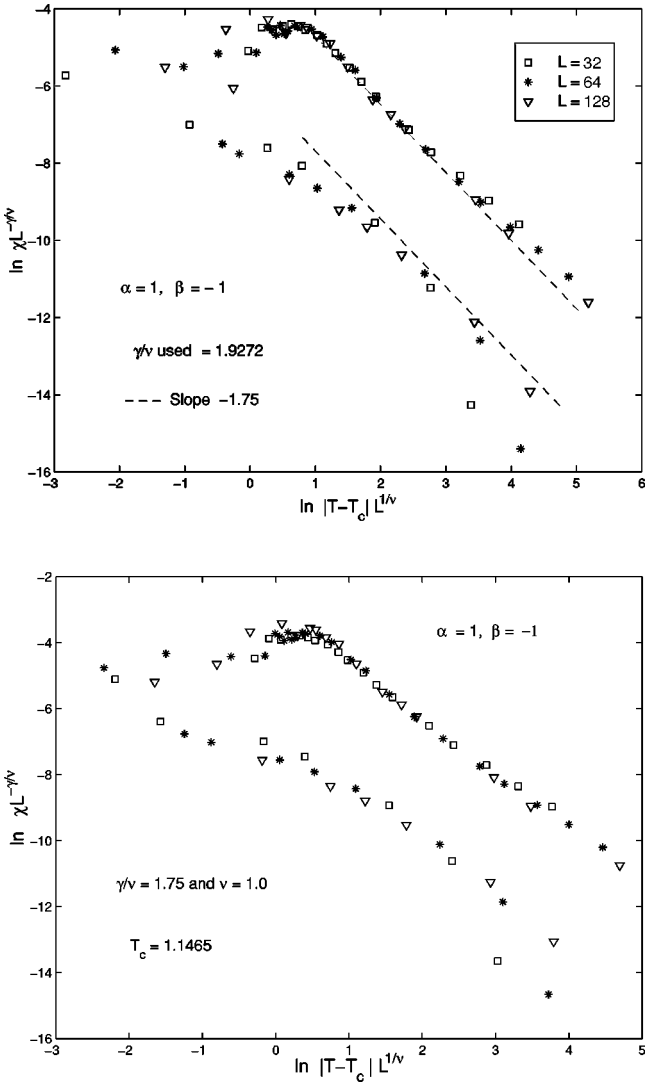

FIG. 7. Data collapse plot for the case of $\alpha=1$, $\beta=-1$. Top plot uses γ/ν obtained ''experimentally'' while the bottom plot assumes it to be 1.75. Both plots assume γ to be 1.75. The T_c value used for the first plot was 1.1487 taking ν to be 0.9081 while it was 1.1465 for $\nu=1$ in the second.

observed that a straight line of slope 1.75 can be fitted through the data points in the linear regions. Thus, the assumption of γ being 1.75 is consistent with the plots. Further, we observed that the data points for different system sizes show signs of scaling behavior, in that data points from smaller systems deviate from the perceived linear region faster. This is true for both the top and bottom branches and is mainly due to finite-size effects. Another point to note is the very short linear regions obtained from the model. Finally, compare the top plot with the bottom in Fig. 7 where the exponents assume Ising values. The data collapse in the bottom plot near the ''bend'' is not as good as in the top plot.

Similar situations occurred for the other settings of β. All the slopes measured are close to the value of 1.75 assumed. Again, collapse is visually better with the all-experimental cases.

We also moved on to look at the case where α is larger than 1. It was found that the quality of data collapse is poorer. Does this imply that the deviation from the Ising

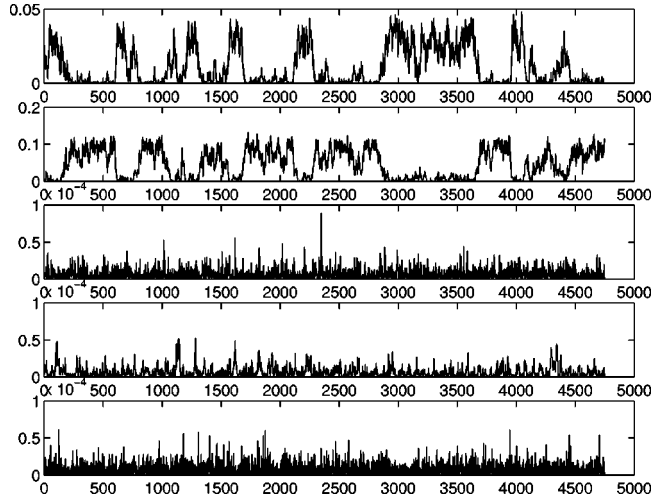

FIG. 8. Fluctuations of $|\tilde{n}|^2$ with time near T_c for the driven system. Parameters: $\beta=-10$, $\alpha=1$, $L=128$, and $T=1.2405$. The quantities plotted on the y axes are (from top to bottom) $|\tilde{n}(0,1,1)|^2$, $|\tilde{n}(0,0,1)|^2$, $|\tilde{n}(0,2,0)|^2$, $|\tilde{n}(0,1,0)|^2$, and $|\tilde{n}(0,4,0)|^2$, as in Fig. 4. The horizontal time axis is in units of 200 MCS. Note that as the value in the second row (FE) increases, that in the first row decreases, and vice versa.

model is more severe for this case? It is hard to make any statements as current knowledge indicates that intralayer couplings are not expected to affect the universality class of the model system. However, although $\beta=-10$ gave us a γ/ν ratio of 1.9268, that of $\beta=-1$ is only 1.7939, which is still a puzzle. As the susceptibility plots from $\alpha=2$ are similar in nature to those from $\alpha=1$, we do expect similar results, though the peak heights are lower in the former case (see Fig. 9 below). We suspect that more data points are needed near T_c for the $\alpha=2$ cases.

VII. DISCUSSION AND SPECULATION

Though our numerical results indicate non-Ising behavior, there may still be problems. The observed peaks are increasing at a rate higher than expected for the Ising model as L increases and we do not see any reasonable way to bring down the peak heights. The phenomenon of critical slowing down may be affecting our numerical results. However, the huge demand on computer resources constrained us to 10^6 MCS per run for the three system sizes we looked at.

For equilibrium systems approaching criticality, the appropriate part of the power spectrum we are monitoring (whose time average is the order parameter) is quite constant but with sudden drops to zero (the top two plots in Fig. 8). (Note that the drops as depicted are not as sudden, since we sample the data only every 200 MCS.) Going even closer to criticality, we saw only ''ridges'' and ''valleys.'' These are the huge fluctuations of the dominant power spectrum (that for the FE phase in our case) expected due to divergence of the susceptibility. For Ising systems, all other entries should be near zero. Hence for the equilibrium FE-D transition, only χ_{FE} diverges near criticality.

For the driven case, the story is quite different. When drops occur for the FE representation, the entry for AFS (stripped antiferromagnetic layers) rises. They are in a way

antagonistic to each other. What we are seeing here is that, instead of the system going into a state with no discernible structure when it looks less FE-like, the particles *collectively* form a phase that is like the pure AFS phase, possible only under the drive. It is a situation where the FE-D-FE state during a simulation run at a T close to T_c is replaced by FE-AFS-FE.

We can attempt to examine the physics of the situation. During a simulation run at moderately high T, particles from the filled layer may hop onto the empty one (note that the driving field does not influence particle hops across layers). Without any drive, these clumps of particles in a generally particle poor region would not have any long ranged order. However, under the drive, linear interfaces would tend to result due to particle alignment with the external field. Thus a phase resembling the AFS results whenever the FE phase is ''eroded.'' Locally the rule of having particle-hole pairs across layers was satisfied by both FE and AFS phases. In fact, the AFS phase is only slightly higher in energy compared with the FE and is in fact a local minimum solution while FE is the global one. This ability of the lattice gas to switch between two phases of very close energy does not have a counterpart in the equilibrium model.

We thus see that enroute to a disordered configuration as T increases, the FE and AFS phases are both present in the intermediate configuration. Although the negatively coupled bilayer system is FE at moderately low temperatures, as T_c is approached the AFS phase becomes significant whenever the configuration becomes less FE-like. As T is increased further, the amplitudes of both components are observed to become comparable until they both become close to zero (as for other phases) at very high T. We thus may not have a simple FE-D transition but instead a FE/AFS-D transition. Hence the numerical results obtained based on χ_{FE} alone may not give us the full picture. Looking back at the scaling plots, we begin to wonder if the poor collapse near T_c is the result of not taking the AFS phase into account.

Plotting the susceptibility curves for each set of parameter settings over the different system sizes, we found plots characteristic of second-order phase transitions (Fig. 9). However, comparison with Ising plots shows the peaks to skew toward smaller T as L increases, which is a curious observation at this stage.

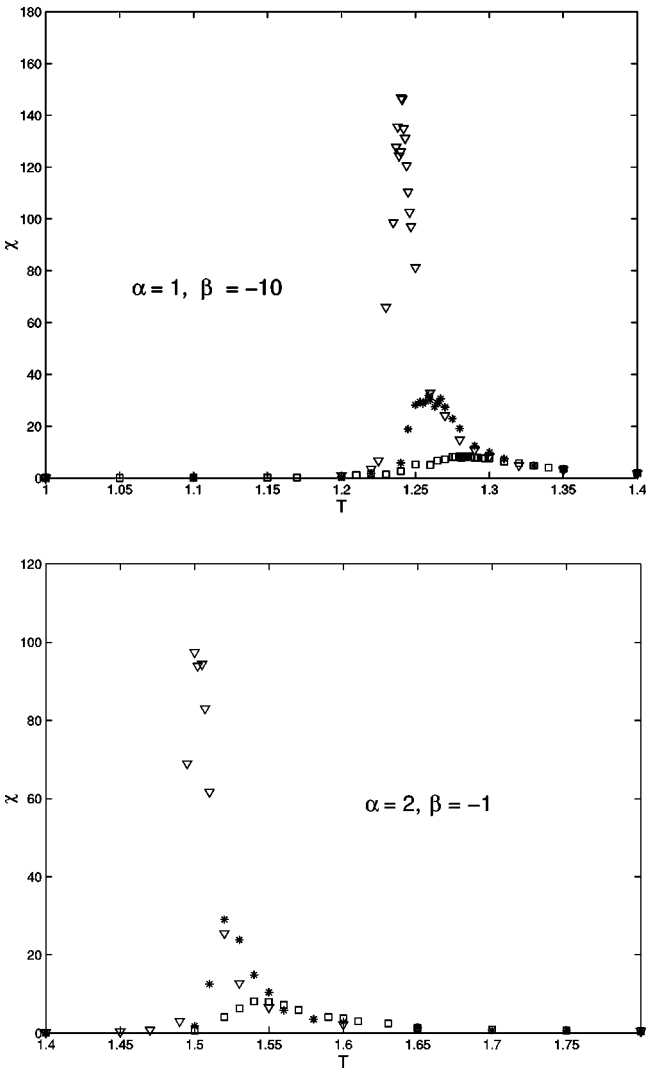

FIG. 9. Selected combined susceptibility plots for $\alpha=1$ and $\alpha=2$.

VIII. CONCLUSIONS

We have attempted to extend the phase diagrams of the bilayer driven lattice gas for unequal intralayer attractive couplings. This is in continuation of the work done by Hill *et.al* [4]. The main findings are that the phase region occupied by the configuration that consist of ferromagnetic bands across the layers (S phase) increases at the expense of the other phase, which is the FE (filled-empty) phase. We speculate that the preference for the S phase over the FE phase by the driving field increases as the intralayer coupling transverse to the drive increases.

We also tried to determine the universality class of our bilayer driven lattice model with repulsive interlayer interactions. Starting with an Ising hypothesis, we found discrepancies for γ/ν with the Ising value of 1.75, obtaining a value closer to 2.0 instead. Hence we have a situation where γ/ν is non-Ising but γ could remain Ising.

Two dominant phases near criticality, namely, the FE and AFS, are observed. The AFS phase comes into play only close to criticality as well as at low temperatures, while the FE phase is dominant at moderate T. All our results were based on FE-D transitions but the true picture could be FE/AFS-D transitions. Essentially, we suspect that a different χ has to be synthesized from χ_{FE} and χ_{AFS}, where the latter may diverge near criticality as well. At this stage, a plausible theory has yet to be worked out. This may explain the poor data collapse near T_c, though whether this susceptibility could give Ising behavior is inconclusive.

Another possibility for non-Ising results could be that the scaling is anisotropic, requiring two correlation length exponents $\nu_\perp$ and $\nu_\parallel$, associated with the directions perpendicular and parallel to the driving field, respectively. This could also explain the nonlinearity of the T_{peak} plots. However, as is well acknowledged in the field, this proposal would be very difficult to investigate.

Thus, it is concluded that the repulsive interlayer DLG does not belong to the Ising class. The theoretical and practical ramifications could be subjects for further research.

[1] S. Katz, J. L. Lebowitz, and H. Spohn, Phys. Rev. B **28**, 1655 (1983); J. Stat. Phys. **34**, 497 (1984).

[2] B. Schmittmann and R. K. P. Zia, *Statistical Mechanics of Driven Diffusive Systems*, Vol. 17 of *Phase Transitions and Critical Phenomena*, edited by C. Domb and J. L. Lebowitz (Academic Press, New York, 1995).

[3] A. Achahbar and J. Marro, J. Stat. Phys. **78**, 1493 (1995).

[4] C. C. Hill, R. K. P. Zia, and B. Schmittmann, Phys. Rev. Lett. **77**, 514 (1996); B. Schmittmann, C. C. Hill, and R. K. P. Zia, Physica A **239**, 382 (1997).

[5] J. Marro, A. Achahbar, P. L. Garrido, and J. J. Alonso, Phys. Rev. E **53**, 6038 (1996).

[6] R. K. P. Zia, L. B. Shaw, and B. Schmittmann, e-print cond-mat/9911035.

[7] L. B. Shaw, B. Schmittmann, and R. K. P. Zia, J. Stat. Phys. **95**, 981 (1999).

[8] J. Marro and A. Achahbar, J. Stat. Phys. **90**, 817 (1998).